Soil Biology and Biochemistry 167 (2022) 108600

Contents lists available at ScienceDirect

Soil Biology and Biochemistry

journal homepage: www.elsevier.com/locate/soilbio

Lithologic control of microbial-derived carbon in forest soils

Peilei Hu [a,b,c], Wei Zhang [a,b,c,**], Hongsong Chen [a,b,c], Lin Xu [a,b,e], Jun Xiao [a,b,c], Yiqi Luo [d], Kelin Wang [a,b,c,*]

[a] Key Laboratory of Agro-ecological Processes in Subtropical Region, Institute of Subtropical Agriculture, Chinese Academy of Sciences, Changsha, China
[b] Huanjiang Observation and Research Station for Karst Ecosystems, Huanjiang, China
[c] Guangxi Industrial Technology Research Institute for Karst Rocky Desertification Control, Nanning, China
[d] Center for Ecosystem Science and Society, Northern Arizona University, Flagstaff, AZ, 86011, USA
[e] College of Resources and Environment, Qingdao Agricultural University, Qingdao, China

ARTICLE INFO

Keywords:
Carbon sequestration
Microbial necromass
Particulate organic matter
Mineral-associated organic matter
Climatic gradient
Bedrock

ABSTRACT

Microbial necromass carbon (MNC) is an important contributor to soil organic carbon. The influence of lithology on MNC remains unclear. MNC is often regarded as a stable, uniform entity, but little consideration has been given to its unprotected and protected fractions. We measured MNC contents in particulate organic matter, which represents the unprotected fraction, and in mineral-associated organic matter, which represents the protected fraction, in forest soils over limestone and clastic rock across a climatic gradient in southwest China. Additionally, nearby croplands with long-term soil tillage were selected for comparison. On average, the contents of protected and unprotected MNC were 52–56% greater in forest soils over limestone compared to clastic rock. Both MNC fractions over clastic rock decreased with increasing the mean annual temperature (MAT), whereas only the unprotected fraction decreased with increasing the MAT over limestone. MNC was regulated by iron oxides and microbial biomass in clastic rock and by exchangeable calcium, iron oxides, and microbial biomass in limestone. However, long-term soil tillage minimized the influences of lithology on MNC. By extrapolating the data to the three provinces of southwest China based on the land-use conversion scenario, we estimated that the existing forestation (recovery and afforestation) has the potential to increase microbial-derived carbon by 17 Tg in topsoil (0–15 cm) over limestone and 11 Tg over clastic rock. The lithology-dependent drivers of microbial-derived carbon accumulation and stability should be considered to predict soil carbon dynamics and minimize carbon emissions under changing environments.

1. Introduction

Due to the crucial role of soil organic carbon (SOC) in regulating climate change and soil fertility and erosion (Davidson and Janssens, 2006; Bossio et al., 2020), promoting SOC accumulation has become a worldwide consensus (Smith et al., 2019). Soil microorganism-mediated processes play a central role in controlling SOC dynamics since soil carbon decomposition, transformation, and stabilization are ultimately the result of microbial activity and growth (Liang et al., 2019). Microorganisms not only reduce SOC stocks via microbial respiration of CO_2, but also increase SOC accumulation via stabilization of microbial necromass (Liang et al., 2017).

Recent evidence suggests that microbial necromass carbon (MNC), also known as microbial-derived carbon, is an important contributor to SOC (Liang et al., 2019). A high proportion of MNC in SOC pools possibly indicates that more carbon is being stored with long-lasting persistence (Zhu et al., 2020). However, the contribution of MNC to SOC has been found to vary widely, ranging from 10% to 62% across study areas (Liang et al., 2019; Fan et al., 2021); this impedes the inclusion of MNC in the Earth System Modeling Framework. Furthermore, there has been no consensus on the patterns and determinants of MNC across different climatic regions (Liang and Balser, 2012; Chen et al., 2020; Yang et al., 2020a). The inconsistent patterns may be attributed to the differences in surficial lithology among the study regions. The

* Corresponding author. Key Laboratory of Agro-ecological Processes in Subtropical Region, Institute of Subtropical Agriculture, Chinese Academy of Sciences, Changsha, China
** Corresponding author. Key Laboratory of Agro-ecological Processes in Subtropical Region, Institute of Subtropical Agriculture, Chinese Academy of Sciences, Changsha, China
E-mail addresses: zhangw@isa.ac.cn (W. Zhang), kelin@isa.ac.cn (K. Wang).

https://doi.org/10.1016/j.soilbio.2022.108600
Received 24 December 2021; Received in revised form 6 February 2022; Accepted 8 February 2022
Available online 10 February 2022
0038-0717/© 2022 Elsevier Ltd. All rights reserved.

lithology of parent materials is a key property of the Earth's critical zone (Hartmann et al., 2012). Lithology has been reported to greatly influence plant community composition and productivity (Jiang et al., 2020), soil geochemistry and properties (Gray et al., 2016), as well as soil microbial communities (Weemstra et al., 2020), which may consequently affect MNC. Thus, the effect of edaphic and climatic factors on the accumulation of MNC may be constrained by surficial lithology. Although a recent study reported different responses of MNC to lithology types (Bhople et al., 2021), whether and how lithology controls the climatic pattern of MNC remain unclear.

In limestone regions, the bedrock composition primarily consists of highly soluble components and can easily be dissolved by rainwater, resulting in low vegetation productivity, discontinuous soils, and thin soil layers, which are highly vulnerable to agricultural activities (Wang et al., 2019). These regions had experienced severe vegetation degradation and rocky desertification as a result of intense human activity but are now among the global hotspots of "Greening Earth" and represent an extensive carbon sink due to massive forestation (recovery and afforestation) (C. Chen et al., 2019; Tong et al., 2020). Clastic rock is usually interwoven with limestone in the same region, and a low percentage of soluble components in clastic rock leads to relatively thick and continuous soils. Additionally, compared with clastic rock, limestone soils are characterized by higher pH, Ca content, and microbial biomass carbon (MBC), which are beneficial to SOC accumulation (Wang et al., 2019). In particular, Ca generally dominates the role of reactive iron (Fe) oxides in protecting SOC from decomposition in limestone soils (Rowley et al., 2018). Although the differences in SOC content between limestone and clastic rock have been identified (Li et al., 2017; Chen et al., 2018), the sequestration strategies of MNC in soils underlain by the two contrasting lithologies and their responses to climatic factors have rarely been explored.

Furthermore, MNC is not a uniform entity. Microbes generally live on the surface of soil particles, and microbial necromass is expected to be protected once it is associated with mineral surfaces, which stabilizes the necromass against microbial decomposition (Craig et al., 2018; Cotrufo et al., 2019; Liang et al., 2019). However, not all microbial necromasses interact with soil minerals, and the unprotected fraction decomposes much more rapidly than the protected fraction (Wang et al., 2020; Fan et al., 2021). Therefore, identifying the contents of unprotected and protected MNC would facilitate a more accurate prediction of microbial-derived carbon dynamics and better management practices to avert soil carbon loss. Despite the different biochemical compositions of microbial cell wall components, Wang et al. (2020) found that fungal, bacterial, and actinobacterial necromass had similar decomposition patterns. Thus, the classification of bacterial and fungal necromass may not reflect the stability of MNC. Conceptualizing soil organic matter (SOM) into mineral-associated organic matter (MAOM) and particulate organic matter (POM) frameworks has been considered an efficient way to identify the drivers of SOM under global change scenarios (Lavallee et al., 2020; Lugato et al., 2021). Owing to mineral protection, microbial necromass in MAOM possibly decomposed much more slowly than that in POM (Lavallee et al., 2020). Thus, we aimed to measure MNC content in MAOM to represent the protected microbial-derived carbon fraction and in POM to represent the unprotected fraction.

In this study, we used amino sugars as a biomarker of the microbial necromass and compared the MNC in soil POM and MAOM fractions and their controlling parameters in forest ecosystems across a broad climatic gradient underlain by limestone and clastic rock. We also compared forests with nearby croplands (long-term soil disturbance) over both lithologies. We hypothesized that: (1) MNC in POM and MAOM fractions and their contribution to organic carbon will be higher in forest soils underlain by limestone than those by clastic rock; and (2) the patterns and controlling factors of MNC along the climatic gradient varied between the two lithologies due to the substantial differences of the soil minerals among them. Our findings advance the understanding of the potential mechanisms of MNC accumulation and emphasize the importance of lithology in MNC modulation.

2. Materials and methods

2.1. Study site description

The study site (22°20′–27°33′ N, 104°46′–108°38′ E) was located along a northwest to southwest transect in the Guizhou and Guangxi provinces of southwest China (Fig. 1). This region is characterized by numerous karst geological formations. It is among the largest continuously exposed carbonate rock areas worldwide, which are unique in terms of multiple physicochemical properties, including high soil Ca and Mg contents, high soil pH, and shallow soil depth (Wang et al., 2019). The lithology of the karst site primarily comprises limestone, followed by dolomite and mixtures of limestone and dolomite, while the lithology of the non-karst area in the same region is primarily clastic rock, which is usually rich in Si and has low soil pH and Ca. The elevation of the study site ranges from 146 m in the southwest to 2233 m in the northwest. Consequently, the temperature in the area decreases from southwest to northwest. The study site has a typical subtropical monsoon climate with mean annual precipitation (MAP) of 1013–1607 mm year^{-1} and mean annual temperature (MAT) of 12.6–21.8 °C.

2.2. Experimental design and soil collection

Soil samples were collected from seven counties along the northwest to southwest transect. The sample areas were located over limestone and clastic rock in the seven counties (Fig. 1). We selected forests estimated to be 60 ± 5 years old in both lithologies in each county with three replicates. The plot characteristics and dominant species of these forests are presented in Table S1. For comparison, croplands over limestone and clastic rock were also selected near each forest plot. The cropland sites that were selected had been cultivated with maize for at least 60 years. The land-use histories of the selected forests and cropland sites were obtained from local forestry administrations. The slope gradient was generally 15–20°. In total, we selected 84 sampling sites (two land-use types × two lithologies × three replicates × seven counties).

We conducted field investigations and collected soil samples between August and October 2018. A 30 × 30 m plot was established at each sampling site. Mineral soil samples (0–15 cm depth) were collected at each plot after removing the organic layer. Soil bulk density was determined by collecting soil in a steel ring with 10 replicates and weighing each replicate after oven drying to a constant weight. In each plot, 20 soil cores with a diameter of 38 mm were collected and pooled as one composite sample. Visible roots and stones were removed with tweezers and stored separately, then the soils were passed through a 2-mm mesh sieve. The coarse particle content (>2 mm, %) was recorded in each composite soil sample. A portion of the fresh soil samples was immediately placed in an icebox in the field, shipped to the laboratory, stored in a refrigerator at 4 °C, and then used for MBC and microbial biomass nitrogen (MBN) analyses. Another portion was used to separate POM and MAOM fractions and measure the SOC and amino sugar content in each fraction. The remaining portion was subjected to analyses to estimate bulk SOC and soil physicochemical properties.

Soil depth and bedrock outcrop ratio (BOR) in each plot were recorded as described by Hu et al. (2018). Briefly, soil depth was measured using a chain pin (length: 100 cm; diameter: 1.2 cm) with 30 replicates inserted vertically into the soil profile until reaching the bedrock. The BOR was estimated by dividing the number of grids over the rock by the total number of grids.

2.3. Size fraction and analysis of SOC and soil amino sugars

After aggregate dispersion, we fractioned SOM into POM and MAOM (Cotrufo et al., 2019). Briefly, 10 g of air-dried soil was dispersed in a sodium hexametaphosphate solution (5 g L^{-1} and 30 mL) and shaken in

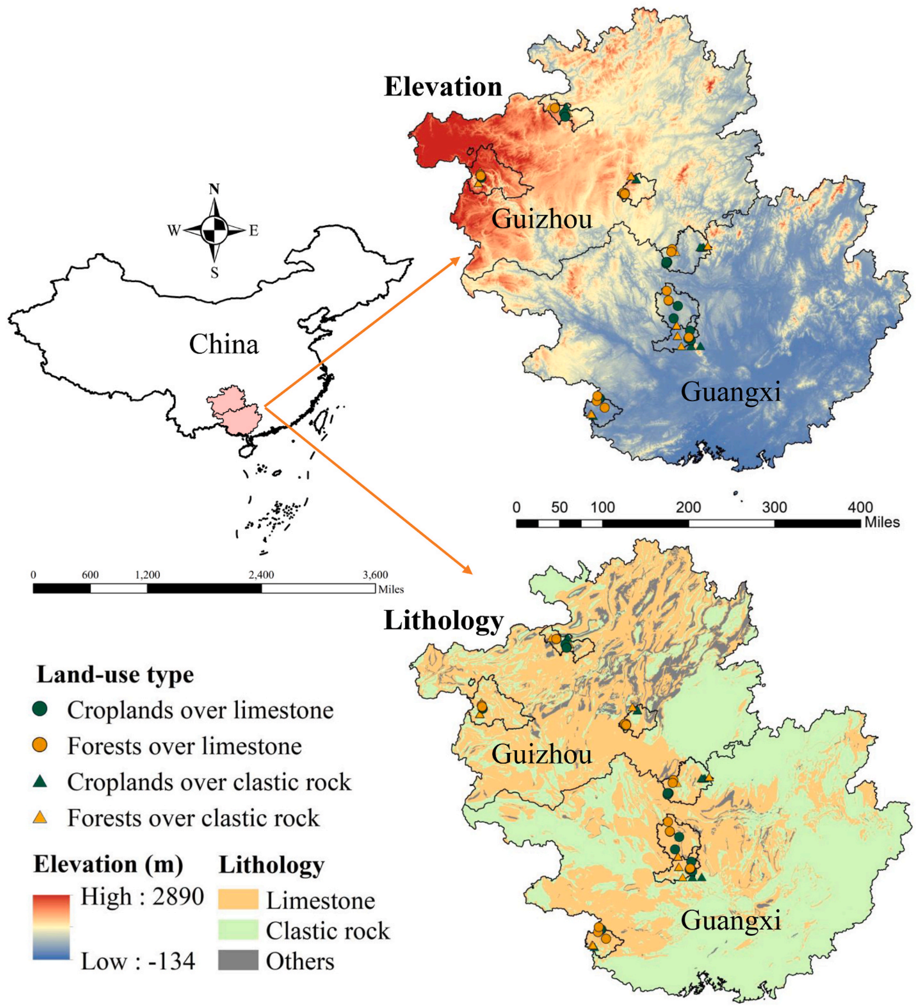

Fig. 1. Spatial distribution of field sampling sites in soils over limestone and clastic rock in Southwest China.

a reciprocating shaker for 4 h. The dispersed soil suspension was rinsed several times with distilled water and then passed through a 53-μm mesh. We considered all materials that remained on the mesh as POM and the fraction that passed through as MAOM. The POM and MAOM fractions were dried at 55 °C to a constant weight and then used to measure the contents of SOC and MNC in each fraction.

SOC in both fractions was measured via wet oxidation using the dichromate redox colorimetric method (Nelson and Sommers, 1996). MNC in each soil fraction was assessed by analyzing the amino sugars (Chen et al., 2021). Briefly, 0.15 g of oven-dried soil (after being passed through a 0.15-mm mesh sieve) was hydrolyzed with 10 mL of 6 M HCl at 105 °C for 8 h. The solution was then filtered, adjusted to pH 6.6–6.8, centrifuged, and freeze-dried. Methanol (5 mL) was added to dissolve the residues, following which, the solution was dried with nitrogen gas at 45 °C. The dried residues were dissolved in deionized water (0.5 mL), dried again with nitrogen gas, and then redissolved in 2 mL of deionized water. After the pre-column derivatization procedure with ortho-phthaldialdehyde, amino sugar concentrations were determined using a high-performance liquid chromatographer (Dionex Ultimate 3000, Thermo Fisher Scientific) equipped with a silica gel column (Kromasil C18; 250 mm × 4.6 mm, 5 μm). Individual amino sugars, including muramic acid (MurA) and glucosamine (GluN), were identified and quantified. MurA was used as a biomarker for bacterial necromass. Because GluN is present in both bacterial and fungal cell walls, fungal-derived GluN was calculated according to the molar ratio of GluN to MurA of 2:1 in bacterial cell walls (Yuan et al., 2020). Fungal and bacterial MNC was calculated as follows:

$$\text{F-GluN } (\mu g\ g^{-1}) = \text{total GluN } (\mu g\ g^{-1}) - 2 \times \text{MurA } (\mu g\ g^{-1}) \times (179.2/251.2)$$

$$\text{Fungal MNC } (g\ kg^{-1}) = \text{F-GluN} \times 9/1000$$

$$\text{Bacterial MNC } (g\ kg^{-1}) = \text{MurA} \times 45/1000$$

where F-GluN is the fungal-derived GluN; 179.2 is the molecular weight of GluN, and 251.2 is the molecular weight of MurA; 9 is the conversion value of F-GluN to fungal MNC, and 45 is the conversion value of MurA to bacterial MNC; and 1000 is the conversion factor for μg g^{-1} to g kg^{-1}. The total MNC was calculated as the sum of the fungal and bacterial MNC.

2.4. Soil microbial biomass and physicochemical properties

Fresh soil was used for MBC and MBN analyses using the chloroform fumigation-extraction method (Wu et al., 1990). SOC content in bulk soil was measured using the same method utilized to determine organic carbon in the POM and MAOM fractions. The total nitrogen (TN) content in the bulk soil was measured using an elemental analyzer (Vario MAX, Elementar, Germany). The stoichiometric imbalance between resource and microbial biomass (i.e., C:N imbalance) was calculated as the ratio of soil C:N (the ratio of SOC to TN) to MBC:MBN (Takriti et al., 2018).

Soil pH was measured using a pH electrode (FE20K, Mettler-Toledo, Switzerland) with a 1:2.5 soil to water suspension. Soil exchangeable Ca (Ca^{2+}) and Mg (Mg^{2+}) were displaced via compulsive exchange in ammonium acetate (1 mol L^{-1}) at pH 7.0 and were then analyzed using ICP-OES (Agilent, Santa Clara, USA), and values were reported as cmol kg^{-1}. Free iron oxides (Fe_d) represent the amount of pedogenic Fe within oxides, silicates, and organic complexes, whereas amorphous iron oxides (Fe_o) originate from poorly crystalline mineral complexes (L. Chen et al., 2019). Soil Fe_o contents were determined by the acid oxalate extraction method and Fe_d contents by the citrate-bicarbonate-dithionite method, and both were analyzed by ICP-OES (Agilent, Santa Clara, USA). Soil texture was measured using a laser diffraction particle size analyzer (Mastersizer 2000; Malvern, UK) after the removal of carbonates by hydrochloric acid and SOM by hydrogen peroxide.

2.5. Climate and plant biomass carbon

The MAT and MAP of the sampling sites were obtained from maps produced by the National Meteorological Information Center of China (http://data.cma.cn/). The plant aboveground biomass carbon (ABC, Mg C ha^{-1}) and belowground biomass carbon (BBC, Mg C ha^{-1}) for each sampling forest site were extracted from a global aboveground and belowground standing biomass carbon density dataset developed by Spawn et al. (2020). The dataset is publicly available and can be accessed through the Oak Ridge National Laboratory DAAC data repository (https://doi.org/10.3334/ORNLDAAC/1763). These data were then imported into ArcGIS 10.5, and MAT, MAP, and plant biomass carbon were extracted for each site using the longitude and latitude values of the sampling sites.

2.6. Soil carbon stock calculation

Increased SOC and MNC stocks under the existing forestation scenario in the three provinces of southwest China were calculated using the following equation:

$$T_{increase} = (C_{forest} \times BD_{forest} \times (1-\delta_{forest}) - C_{cropland} \times BD_{cropland} \times (1-\delta_{cropland})) \times 15 \times (1\text{-BOR}) \times S/10$$

where $T_{increase}$ represents the increase in total SOC or MNC (Tg); C_{forest} represents SOC or MNC contents in forests, and $C_{cropland}$ represents SOC or MNC contents in croplands (g kg^{-1}); BD_{forest} is the soil bulk density in forests, and $BD_{cropland}$ is the soil bulk density in croplands (g cm^{-3}); δ_{forest} represents the coarse particle content (>2 mm, %) in forests, and $\delta_{cropland}$ represents the coarse particle content in croplands; 15 is the soil depth (cm); BOR is the bedrock outcrop ratio (%). S is the area of forestation from 2000 to 2017 (Mha) in the three provinces of southwest China; 10 is used for unit conversion.

2.7. Statistical analysis

Data were tested for normal distribution and homogeneity of variance; when required, data were natural log-transformed to satisfy these criteria. A one-way analysis of variance was used to test the differences in the response variables between lithologies within the same land-use type or between land-use types within the same lithology. Statistical analyses were performed using SPSS 18.0 (SPSS Inc., Chicago, USA), and figures were plotted using OriginPro 2021 (OriginLab, Hampton, USA).

First, the effects of the explanatory variables on the MNC content in the POM and MAOM fractions were assessed using random forest analysis. Climatic factors (MAT and MAP), plant biomass carbon (ABC and BBC), soil variables (pH, C:N ratio, Ca^{2+}, Mg^{2+}, Fe_o, Fe_d, and the ratio of clay to sand), and soil microbial variables (MBC and C:N imbalance) were selected to identify the relative importance of a given variable compared to the other variables. The percentage increase of the mean squared error (%IncMSE) was used to rank the relative importance of the explanatory variables with the "randomForest" package, and the significance of the effect of each explanatory variable on MNC was estimated using the 'rfPermute' package in R 4.0.2 (Chen et al., 2021). Second, regression analysis was used to further explore the relationships between the selected explanatory and response variables and was performed using OriginPro 2021 (OriginLab, Hampton, USA).

The direct and indirect effects of the selected explanatory variables on the MNC in the POM and MAOM fractions were evaluated using structural equation modeling (SEM). To simplify the model, MAT; the soil variables pH, Ca^{2+}, and Fe_o; and the microbial variable MBC were selected based on random forest and regression analyses. An initial metamodel was constructed for evaluation based on prior knowledge (Fig. S1). For simplicity, we first removed the least significant path, re-estimated the model, and then removed the next least significant path, and so on, until finally, all remaining paths in the SEM were significant (Wang et al., 2021). The SEM analysis was calculated using maximum-likelihood estimation, and the goodness of fit was evaluated using chi-squared values (χ^2), probability level (p), root mean square error of approximation (RMSEA), and goodness-of-fit index (GFI). Furthermore, as sample size may pose issues for SEM application, the fit of the model was confirmed using Bayesian analysis. The SEM analysis was performed using Amos 24 (Amos Development Corporation, Chicago, USA).

3. Results

3.1. SOC fractions in soils over limestone and clastic rock

Overall, the bulk SOC content in forest soils over limestone was significantly higher than that over clastic rock by 33% ($p < 0.05$, Fig. 2a). The particulate organic carbon (POC) was also significantly higher by 37% ($p < 0.05$, Fig. 2b). The ratio of POC to SOC was not significantly different between the two lithologies (Fig. 2d). Compared with croplands, forest soils over both lithologies had significantly higher contents of SOC and POC and the ratio of POC to SOC ($p < 0.05$, Fig. 2).

3.2. Soil MNC in POM and MAOM fractions in soils over limestone and clastic rock

Generally, the contents of bacterial, fungal, and total MNC and their contributions had a similar pattern in bulk soil and the two fractions (Figs. 3, 4, S2). Specifically, forest soils over limestone had significantly higher contents of fungal and total MNC both in POM and MAOM fractions than over clastic rock ($p < 0.05$, Fig. 3c,e; Fig. 4c,e). The ratio of fungal MNC to organic carbon in the POM fraction was also significantly higher in forest soils over limestone compared to clastic rock ($p < 0.05$, Fig. 3d). In contrast with fungal MNC, there was no significant difference in bacterial MNC content and their contributions to the corresponding SOC fractions between limestone and clastic rock (Fig. 3a,b; Fig. 4a,b). Additionally, the ratio of fungal to bacterial MNC was higher in forest soils over limestone than over clastic rock ($p < 0.05$, Fig. S3), and 81–87% of total MNC stored in forest soils over limestone was fungal-derived compared to 73–80% over clastic rock.

We also found that the bacterial, fungal, and total MNC contents in POM and MAOM fractions, and their contributions to the corresponding SOC fractions, did not differ significantly between cropland soils over limestone and clastic rock (Figs. 3 and 4).

3.3. Responses of soil MNC to climatic and edaphic factors

We used 13 variables that reflect the effects of climatic factors, plant biomass, soil properties, and microbial parameters to explain the variances of MNC in the POM and MAOM fractions (Fig. S4). Factors controlling MNC in the POM and MAOM fractions differed in forest soils over limestone, whereas the controlling factors were similar over clastic rock (Fig. S4). Overall, MAT, pH, Ca, Fe_o, and MBC were the most important factors controlling the variance in the MNC.

Regression analyses results indicated that the responses of the MNC to climatic and edaphic factors differed between forest soils over

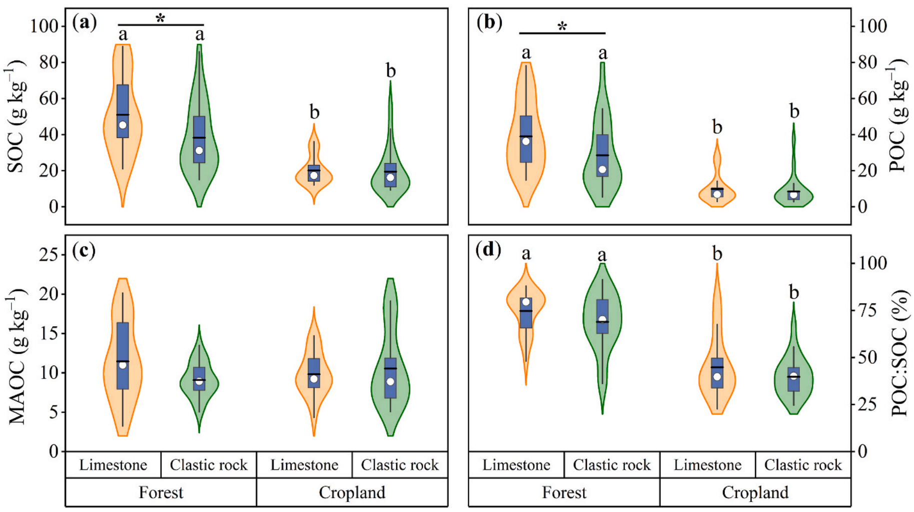

Fig. 2. Contents of bulk soil organic carbon (SOC) (a), particulate organic carbon (POC) (b), mineral-associated organic carbon (MAOC) (c), and the ratio of POC to SOC (POC:SOC) (d) in soils over limestone and clastic rock. The ends of the boxes represent the 25th and 75th percentiles, the white circles represent the medians, and the central black lines represent the means. Lowercase letters represent significant differences at $p < 0.05$ between forests and croplands within the same lithology. * represents significant differences at $p < 0.05$ between limestone and clastic rock within the same land-use type.

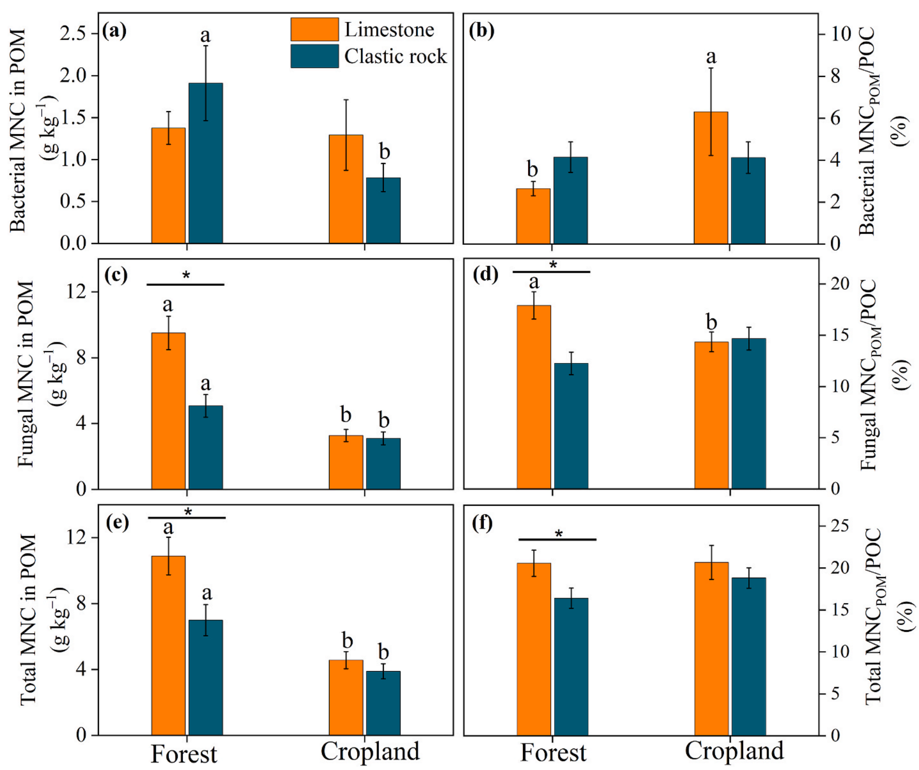

Fig. 3. Contents of soil microbial necromass carbon (MNC) in particulate organic matter (POM) fraction and the ratios of MNC of particulate organic matter (MNC_{POM}) to particulate organic carbon (POC). Bars represent means ± standard errors (n = 21). Lowercase letters represent significant differences at $p < 0.05$ between forests and croplands within the same lithology. * represents significant differences at $p < 0.05$ between limestone and clastic rock within the same land-use type.

limestone and clastic rock (Fig. 5). Specifically, only MNC in the POM fraction decreased with MAT in forest soils over limestone, whereas both MNC in POM and MAOM fractions over clastic rock decreased with MAT (Fig. 5a,f). Soil pH was negatively correlated with only MNC in the POM fraction in the clastic rock sites (Fig. 5b,g). Fe_o was positively correlated with only MNC in the POM fractions in limestone sites, whereas it was positively correlated with both MNC in POM and MAOM fractions in clastic rock sites (Fig. 5d,i). Additionally, Ca^{2+} was positively correlated with MNC in the MAOM fraction in the limestone (Fig. 5c,h). For both lithologies, MNC in the POM and MAOM fractions increased with MBC (Fig. 5e,j).

3.4. Determinants of soil MNC accumulation

The SEM determined using both the maximum-likelihood estimation method and Bayesian analysis showed similar results (Table S2). The SEM results mirrored those that were obtained using regression analyses in that the effects of climatic and edaphic factors on MNC differed between the two lithologies (Fig. 6). Specifically, MAT negatively affected MNC in the POM fraction directly and indirectly (via its effect on Fe_o) in forest soils over limestone, whereas MAT had indirect effects on both MNC in POM and MAOM fractions over clastic rock. Additionally, Fe_o was only directly associated with MNC in the POM fraction in forest soils

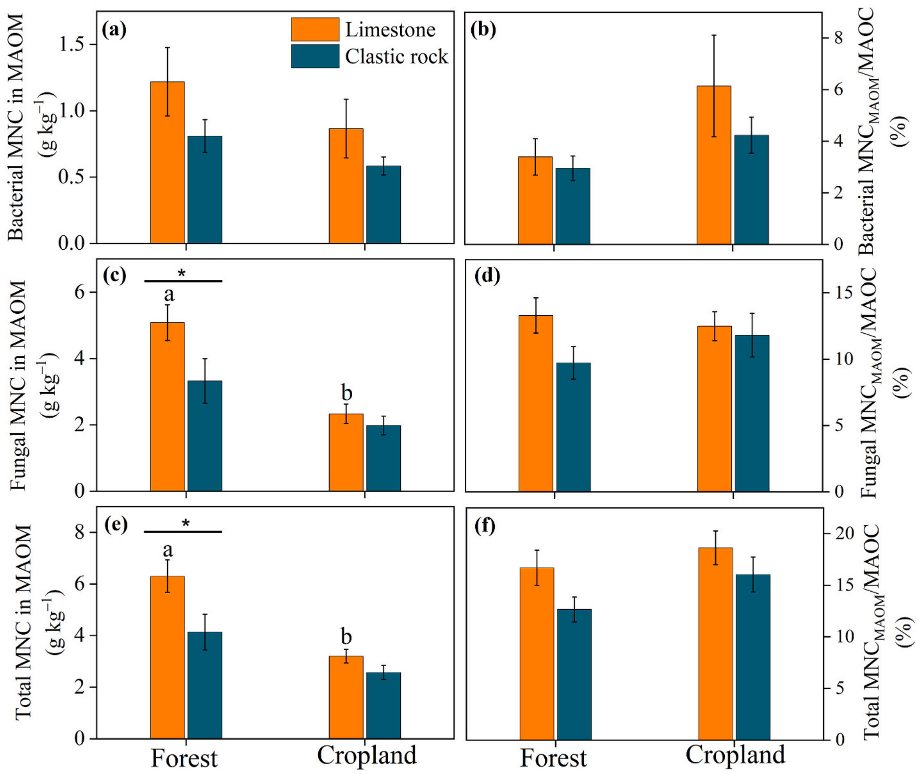

Fig. 4. Contents of soil microbial necromass carbon (MNC) in mineral-associated organic matter (MAOM) fraction and the ratios of MNC of mineral-associated organic matter (MNC_{MAOM}) to mineral-associated organic carbon (MAOC). Bars represent means ± standard errors (n = 21). Lowercase letters represent significant differences at $p < 0.05$ between forests and croplands within the same lithology. * represents significant differences at $p < 0.05$ between limestone and clastic rock within the same land-use type.

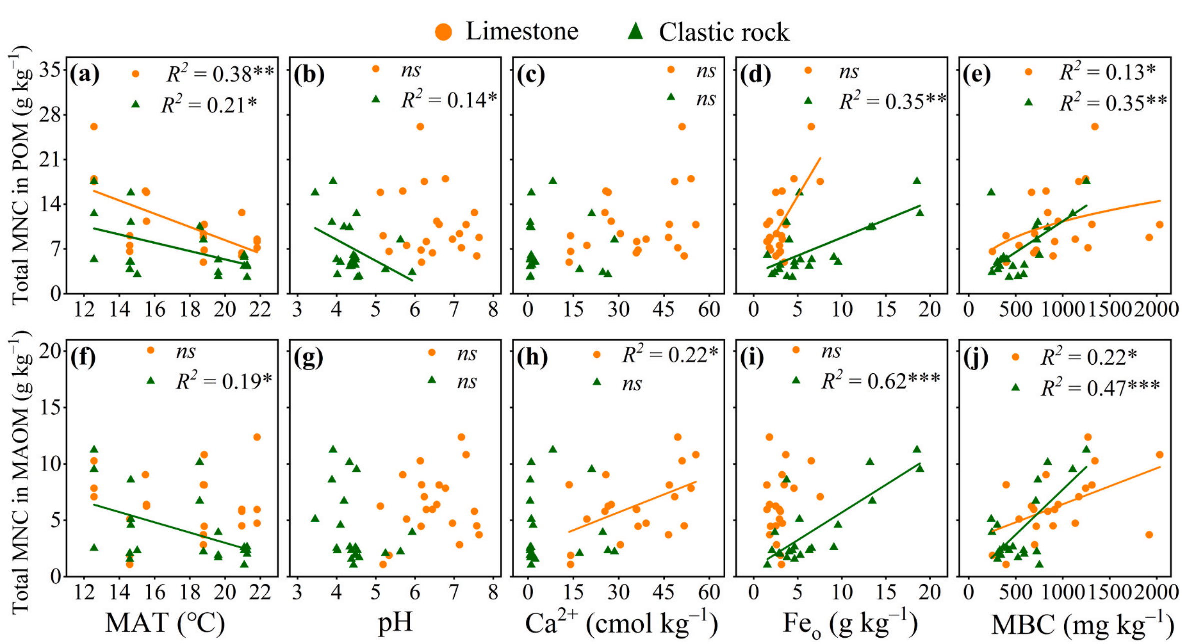

Fig. 5. Relationships of microbial necromass carbon (MNC) in particulate organic matter (POM) and mineral-associated organic matter (MAOM) fractions with climatic and soil variables in forest soils. Linear regression analysis was undertaken between MNC in POM/MNC in MAOM fraction and climatic and edaphic factors separately. MAT, mean annual temperature; pH, soil pH; Ca^{2+}, soil exchangeable calcium; Fe_o, amorphous iron oxides; MBC, microbial biomass carbon. $^{*}p < 0.05$, $^{**}p < 0.01$, and $^{***}p < 0.001$; *ns*, not significant regressions ($p > 0.05$).

over limestone, whereas Fe_o had direct and indirect effects (via its effect on MBC) on both MNC fractions in soils over clastic rock. Compared to soils over clastic rock, Ca^{2+} was an additional factor that indirectly affected MNC in soils over limestone. Similar to the regression analyses, MBC directly and positively affected both the MNC fractions in soils over both lithologies.

4. Discussion

4.1. Lithology effects on unprotected and protected microbial-derived carbon fractions

The results supported our first hypothesis and demonstrated that the contents of both unprotected and protected MNC were significantly

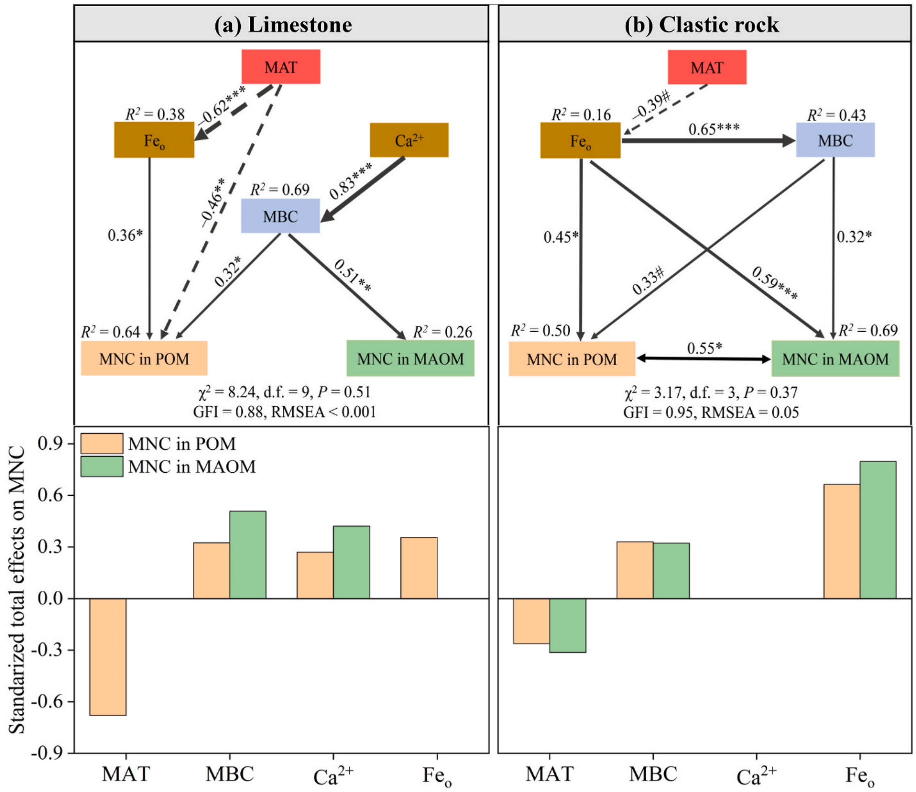

Fig. 6. Structural equation modeling (SEM) showing the dependence of microbial necromass carbon (MNC) in particulate organic matter (POM) and MNC in mineral-associated organic matter (MAOM) fractions from climatic and soil variables in forest soils over limestone (a) and clastic rock (b), and their standardized direct and indirect effects derived from the SEMs. Solid arrows indicate a positive relationship, and dotted arrows indicate a negative relationship. The numbers adjacent to the arrows are the standardized path coefficients, and the arrow width indicates the strength of the standardized path coefficient. R^2 values represent the proportion of the variance explained for each endogenous variable. MAT, mean annual temperature; Fe$_o$, amorphous iron oxides; Ca^{2+}, soil exchangeable calcium; MBC, microbial biomass carbon; χ^2, chi-square values; d.f., degree of freedom; GFI, goodness-of-fit index; RMSEA, the root mean square error of approximation. $^{\#}p < 0.10$, $^{*}p < 0.05$, $^{**}p < 0.01$, $^{***}p < 0.001$.

higher in forest soils over limestone than over clastic rock, which suggests that lithology can strongly regulate microbial-derived carbon accumulation. Although the effects of lithology on SOM have been explored and verified (Doetterl et al., 2015, 2018; Yang et al., 2020b), their controls on microbial-derived carbon have seldom been reported. A recent study found that soil microbial necromass accumulated differently in alpine ecosystems with different bedrock types (Bhople et al., 2021), which confirmed a non-negligible effect of the parent material on microbial necromass.

In our study, both unprotected and protected MNC contents were positively related to MBC (Fig. 6). Although soil microorganisms can decompose SOM, the pool size of microbial biomass is also considered to contribute to MNC through microbial uptake, assimilation, growth, and death (Liang et al., 2017). Thus, the significantly higher MBC content in forest soils over limestone compared to clastic rock (Table S3) suggests greater MNC accumulation. Higher pH and Ca^{2+} concentration in forest soils underlain by limestone were also contributing factors to the higher MNC (Table S3). This is because the higher limestone soil pH favors the growth of fungi and, thus, increases the fungal necromass (Aciego Pietri and Brookes, 2009). This is consistent with our results, which showed a higher ratio of fungal to bacterial MNC in forest soils underlain by limestone compared to clastic rock (Figs. S3a and b). Higher soil Ca^{2+} concentration in limestone improves soil structure, moisture, and aeration, while also favoring the growth of microorganisms (Golchin et al., 1996). In addition, soil Ca^{2+} can stabilize SOM by forming inner- and outer-sphere cation bridges (Rowley et al., 2018) and stabilizes fungal-derived carbon more effectively than bacterial-derived carbon (Six et al., 2006).

4.2. Control over microbial-derived carbon accumulation: lithology dependence

Empirical observations of the responses of unprotected and protected MNC fractions to climatic and edaphic factors across a large scale in soils underlain by different lithologies are scarce. Our results provide quantitative evidence that factors affecting MNC are lithology-dependent and that this dependence also differed between unprotected and protected fractions.

We found that both unprotected and protected MNC fractions in forest soils over clastic rock decreased with increasing MAT. In contrast, in forest soils over limestone, only the unprotected fraction decreased with MAT (Fig. 5a,f), which supports our second hypothesis that the MNC fractions between the two lithologies respond differently to climate. Higher temperatures generally promote the decomposition of MNC (Chen et al., 2020). In our study, warmer temperatures indirectly affected unprotected and protected MNC fractions via the regulation of Fe$_o$ in forest soils underlain by clastic rock (Fig. 6b). Fe$_o$ is more closely related to the stability of soil aggregates than Fe$_d$ (Duiker et al., 2003), and thus is able to decrease microbial necromass decomposition. Additionally, Fe$_o$ has a very large specific surface area, which helps in the adsorption of the microbial biomass component and the stabilization of microbial necromass (Kästner and Miltner, 2018). Thus, higher Fe$_o$ contents promoted the accumulation of microbial-derived carbon (Fig. 6). The negative effect of higher temperatures on Fe$_o$ content (Figs. 6 and S5a) could be because warmer temperatures favor the transformation of Fe$_o$ to other crystalline Fe oxides (Zhao et al., 2016). Therefore, as the temperature increases, the capacity of Fe$_o$ to stabilize microbial-derived carbon decreases.

In contrast to clastic rock, Fe$_o$ and temperature only affected the unprotected MNC fraction in forest soils over limestone but not the protected fraction (Fig. 5d,i, 6a). Compared to clastic rock sites, lower Fe$_o$ content in limestone sites (Table S3) had a limited effect on microbial-derived carbon stability. Instead, Ca^{2+} may outweigh the role of Fe oxides in calcareous soils (Rowley et al., 2018). Specifically, abundant soil Ca^{2+} plays an important role in the stabilization of MNC through inner- and outer-sphere cation bridging (He et al., 2021). Thus, high Ca^{2+} concentration in forest soils over limestone (Table S3) and the negligible effect of warmer temperatures on Ca^{2+} (Fig. S5b) could negate the effect of higher temperatures on the decomposition of the protected MNC fraction. Overall, lithology mediates the climatic pattern of microbial-derived carbon fractions in forest soils through the modification of soil properties.

Soil pH also showed different effects on MNC in forest soils underlain by the two lithologies. Specifically, soil pH was negatively correlated with the unprotected MNC fraction in soils underlain by clastic rock but showed no correlation with MNC in soils underlain by limestone (Fig. 5b,g). The distinctly different soil pH controls on MNC over the lithologies were likely due to the differences in background soil pH. The unprotected MNC fraction decreased with increasing the pH in acidic soils underlain by clastic rock, possibly because the improved microbial living environment promotes the decomposition of unprotected microbial-derived carbon (Leifeld et al., 2008; Luo et al., 2020). The lack of a correlation between MNC and soil pH over limestone was possibly due to the trade-off between increased microbial carbon use efficiency (CUE) and decreased turnover rate with increased soil pH in near-neutral or alkaline soils (Malik et al., 2018). High microbial CUE potentially favors the accumulation of microbial-derived carbon (Cotrufo et al., 2013), whereas the low turnover rates of microbial biomass lead to slow necromass production and, therefore, potentially less microbial-derived carbon (Spohn et al., 2016). Thus, although soil pH was previously considered as an important factor affecting soil microbial physiology parameters and thus their necromass (Wang et al., 2021), its effects varied depending on lithology.

4.3. Implications for soil carbon sequestration

Microbial-derived carbon should not be regarded as a uniform entity as MNC in POM and MAOM fractions respond distinctly to MAT in forest soils over limestone. This result partially aligns with the idea that the unprotected fraction of the microbial necromass could be rapidly decomposed (Fan et al., 2021). We also found that MNC in the POM fraction was more sensitive to MAT than organic carbon in the POM fraction in forest soils over limestone (Figs. S6a and c). Compared to plant-derived carbon, the compounds in MNC tend to be more nutrient-dense and richer in nitrogen (Miltner et al., 2012; Liang et al., 2019), which may require less depolymerization prior to plant or microbial assimilation. Thus, the unprotected fraction could be an important source of nutrients for the growth of microorganisms and plants (Drigo et al., 2012; Morrissey et al., 2015). Overall, these results highlight the need to characterize and quantify unprotected and protected fractions of microbial-derived carbon separately, particularly under future climate change scenarios.

In contrast to forest soils (undisturbed soils), neither the contents of unprotected and protected MNC fractions (Figs. 3 and 4) nor their responses to MAT (Fig. S7) showed significant differences in cropland soils (disturbed soils) between limestone and clastic rock. Tillage in croplands can reduce the physical and chemical protection of SOM (Davidson and Janssens, 2006), which may accelerate the decomposition and loss of MNC. Additionally, removal of the aboveground biomass in croplands reduces carbon inputs, resulting in the reduction of living microbial biomass and thus their residues. Consequently, long-term soil disturbance may obscure and distort the influence of lithology on microbial-derived carbon. This suggests that SOC and MNC contents in limestone soils are high only in the absence of soil disturbance. Therefore, no-tillage management, similar to forestation, on croplands in limestone sites would be an effective strategy to accumulate soil carbon. According to the data extracted from Tong et al. (2020), the areas of forestation (including recovery and afforestation on croplands) from 2000 to 2017 were ~4.35 Mha over limestone and ~5.38 Mha over clastic rock in three provinces of southwest China (Guizhou, Guangxi, and Yunnan). Assuming that forestation would result in a state similar to that of forest ecosystems after several decades (Bastin et al., 2019), we extrapolated the data demonstrating the differences in SOC and MNC densities between forests and croplands (Fig. 7) and bedrock outcrop ratio for both lithologies (Table S4) in the three provinces. We concluded that an increase of 84 Tg, of which 20% is microbial-derived, would occur in the topsoil (0–15 cm) underlain by limestone, while an increase of 86 Tg, of which 13% is microbial-derived, would occur in the topsoil underlain by clastic rock. Considering that forest soils over limestone contain relatively higher pools of MNC that are resistant to warmer temperatures relative to clastic rock, forestation on degraded croplands in limestone sites may be the most effective way to reduce CO_2 efflux from the soil.

Our results imply that ignoring the important role of lithology in regulating microbial-derived carbon will possibly contribute to large inaccuracies in the prediction of the response of soil carbon to a changing climate. However, the effects of climate should not be ignored. The weathering and geochemistry of soil is determined not only by the mineralogical composition of the bedrock, but also by climate (Doetterl et al., 2018). Therefore, we recommend further research that combines the interaction effects of bedrock geochemistry (including bedrock nutrient release) and climate on microbial-derived carbon accumulation.

5. Conclusions

Compared to clastic rock, forests underlain by limestone are more conducive to accumulating both unprotected and protected MNC fractions and are less susceptible to warmer temperatures. Our study provides evidence that lithology affects the contents of MNC fractions and their response to temperature in forest soils, primarily through the regulation of soil minerals and MBC. However, croplands with long-term soil disturbance over both lithologies deplete significant amounts of MNC and increase their vulnerability to warmer temperatures. In the context of the existing forestation in southwest China, an additional 17 Tg of microbial-derived carbon may be sequestered in the topsoil over limestone, and 11 Tg might be sequestered in the case of clastic rock. Overall, our results demonstrate that the key soil minerals governing

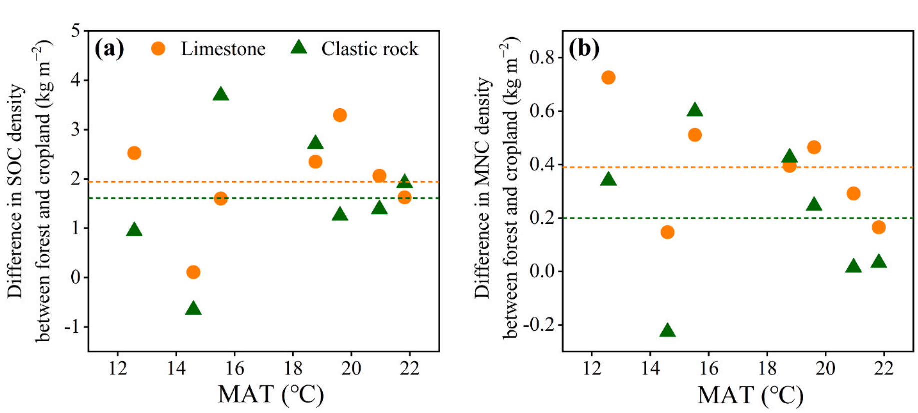

Fig. 7. Differences in soil organic carbon (SOC) (a) and microbial necromass carbon (MNC) densities (b) between forest and cropland in topsoil (0–15 cm) over limestone and clastic rock sites. Orange dash lines represent the average difference in SOC or MNC density in limestone sites, and olive dash lines represent the average difference in SOC or MNC density in clastic rock sites. Difference in SOC or MNC density was calculated based on the contents of SOC or MNC, soil bulk density, coarse particle contents (>2 mm, %), soil depth, and bedrock outcrop ratio. (For interpretation of the references to color in this figure legend, the reader is referred to the Web version of this article.)

microbial-derived carbon accumulation and stability are ultimately regulated by lithology.

Funding

This study was supported by the Joint Funds of the National Natural Science Foundation of China [U20A2011]; the State Key Program of National Natural Science Foundation of China [41930652]; the National Natural Science Foundation of China [32001231, 31870502]; the China Postdoctoral Science Foundation [2020M682585]; and the Natural Science Foundation of Guangxi Province [2020GXNSFBA297016].

Data availability statement

The data that support the findings of this study can be accessed at the Science Data Bank (https://www.scidb.cn/en/s/y22mqq).

Declaration of competing interest

The authors declare that they have no known competing financial interests or personal relationships that could have appeared to influence the work reported in this paper.

Appendix A. Supplementary data

Supplementary data to this article can be found online at https://doi.org/10.1016/j.soilbio.2022.108600.

References

Aciego Pietri, J.C., Brookes, P.C., 2009. Substrate inputs and pH as factors controlling microbial biomass, activity and community structure in an arable soil. Soil Biology and Biochemistry 41, 1396–1405.
Bastin, J.F., Finegold, Y., Garcia, C., Mollicone, D., Rezende, M., Routh, D., Zohner, C.M., Crowther, T.W., 2019. The global tree restoration potential. Science 365, 76–79.
Bhople, P., Keiblinger, K., Djukic, I., Liu, D., Zehetner, F., Zechmeister-Boltenstern, S., Joergensena, R.G., Murugan, R., 2021. Microbial necromass formation, enzyme activities and community structure in two alpine elevation gradients with different bedrock types. Geoderma 386, 114922.
Bossio, D.A., Cook-Patton, S.C., Ellis, P.W., Fargione, J., Sanderman, J., Smith, P., Wood, S., Zomer, R.J., von Unger, M., Emmer, I.M., Griscom, B.W., 2020. The role of soil carbon in natural climate solutions. Nature Sustainability 3, 391–398.
Chen, C., Park, T., Wang, X., Piao, S., Xu, B., Chaturvedi, R.K., Fuchs, R., Brovkin, V., Ciais, P., Fensholt, R., Tømmervik, H., Bala, G., Zhu, Z., Nemani, R.R., Myneni, R.B., 2019. China and India lead in greening of the world through land-use management. Nature Sustainability 2, 122–129.
Chen, G.P., Ma, S.H., Tian, D., Xiao, W., Jiang, L., Xing, A.J., Zou, A., Zhou, L., Shen, H., Zheng, C., Ji, C., He, H., Zhu, B., Liu, L., Fang, J.Y., 2020. Patterns and determinants of soil microbial residues from tropical to boreal forests. Soil Biology and Biochemistry 151, 108059.
Chen, H., Li, D., Xiao, K., Wang, K., 2018. Soil microbial processes and resource limitation in karst and non-karst forests. Functional Ecology 32, 1400–1409.
Chen, L., Liu, L., Qin, S., Yang, G., Fang, K., Zhu, B., Kuzyakov, Y., Chen, P., Xu, Y., Yang, Y., 2019. Regulation of priming effect by soil organic matter stability over a broad geographic scale. Nature Communications 10, 5112.
Chen, X., Hu, Y., Xia, Y., Zheng, S., Ma, C., Rui, Y., He, H., Huang, D., Zhang, Z., Ge, T., Wu, J., Guggenberger, G., Kuzyakov, Y., Su, Y., 2021. Contrasting pathways of carbon sequestration in paddy and upland soils. Global Change Biology 27, 2478–2490.
Cotrufo, M.F., Ranalli, M.G., Haddix, M.L., Six, J., Lugato, E., 2019. Soil carbon storage informed by particulate and mineral-associated organic matter. Nature Geoscience 12, 989.
Cotrufo, M.F., Wallenstein, M.D., Boot, C.M., Denef, K., Paul, E., 2013. The Microbial Efficiency-Matrix Stabilization (MEMS) framework integrates plant litter decomposition with soil organic matter stabilization: do labile plant inputs form stable soil organic matter? Global Change Biology 19, 988–995.
Craig, M.E., Turner, B.L., Liang, C., Clay, K., Johnson, D.J., Phillips, R.P., 2018. Tree mycorrhizal type predicts within-site variability in the storage and distribution of soil organic matter. Global Change Biology 24, 3317–3330.
Davidson, E.A., Janssens, I.A., 2006. Temperature sensitivity of soil carbon decomposition and feedbacks to climate change. Nature 440, 165–173.
Doetterl, S., Berhe, A.A., Arnold, C., Bodé, S., Fiener, P., Finke, P., Fuchslueger, L., Griepentrog, M., Harden, J.W., Nadeu, E., Schnecker, J., Six, J., Trumbore, S., Van Oost, K., Vogel, C., Boeckx, P., 2018. Links among warming, carbon and microbial dynamics mediated by soil mineral weathering. Nature Geoscience 11, 589–593.
Doetterl, S., Stevens, A., Six, J., Merckx, R., Van Oost, K., Casanova Pinto, M., Casanova-Katny, A., Muñoz, C., Boudin, M., Venegas, E.Z., Boeckx, P., 2015. Soil carbon storage controlled by interactions between geochemistry and climate. Nature Geoscience 8, 780–783.
Drigo, B., Anderson, I.C., Kannangara, G.S.K., Cairney, J.W.G., Johnson, D., 2012. Rapid incorporation of carbon from ectomycorrhizal mycelial necromass into soil fungal communities. Soil Biology and Biochemistry 49, 4–10.
Duiker, S.W., Rhoton, F.E., Torrent, J., Smeck, N.E., Lal, R., 2003. Iron (hydr)oxide crystallinity effects on soil aggregation. Soil Science Society of America Journal 67, 606–611.
Fan, X., Gao, D., Zhao, C., Wang, C., Qu, Y., Zhang, J., Bai, E., 2021. Improved model simulation of soil carbon cycling by representing the microbially derived organic carbon pool. The ISME Journal 15, 2248–2263.
Golchin, A., Clarke, P., Oades, J.M., 1996. The heterogeneous nature of microbial products as shown by solid-state ^{13}C CP/MAS NMR spectroscopy. Biogeochemistry 34, 71–97.
Gray, J.M., Bishop, T.F.A., Wilford, J.R., 2016. Lithology and soil relationships for soil modelling and mapping. Catena 147, 429–440.
Hartmann, J., Durr, H.H., Moosdorf, N., Meybeck, M., Kempe, S., 2012. The geochemical composition of the terrestrial surface (without soils) and comparison with the upper continental crust. International Journal of Earth Sciences 101, 365–376.
He, M., Fang, K., Chen, L., Feng, X., Qin, S., Kou, D., He, H., Liang, C., Yang, Y., 2021. Depth-dependent drivers of soil microbial necromass carbon across Tibetan alpine grasslands. Global Change Biology 28, 936–949.
Hu, P.L., Liu, S.J., Ye, Y.Y., Zhang, W., Wang, K.L., Su, Y.R., 2018. Effects of environmental factors on soil organic carbon under natural or managed vegetation restoration. Land Degradation & Development 29, 387–397.
Jiang, Z., Liu, H.Y., Wang, H.Y., Peng, J., Meersmans, J., Green, S.M., Quine, T.A., Wu, X., Song, Z.L., 2020. Bedrock geochemistry influences vegetation growth by regulating the regolith water holding capacity. Nature Communications 11, 2392.
Kästner, M., Miltner, A., 2018. Chapter 5 - SOM and microbes—what is left from microbial life. In: Garcia, C., Nannipieri, P., Hernandez, T. (Eds.), The Future of Soil Carbon. Academic Press, pp. 125–163.
Lavallee, J.M., Soong, J.L., Cotrufo, M.F., 2020. Conceptualizing soil organic matter into particulate and mineral-associated forms to address global change in the 21st century. Global Change Biology 26, 261–273.
Leifeld, J., Zimmermann, M., Fuhrer, J., 2008. Simulating decomposition of labile soil organic carbon: effects of pH. Soil Biology and Biochemistry 40, 2948–2951.
Li, D., Wen, L., Zhang, W., Yang, L., Xiao, K., Chen, H., Wang, K., 2017. Afforestation effects on soil organic carbon and nitrogen pools modulated by lithology. Forest Ecology and Management 400, 85–92.
Liang, C., Amelung, W., Lehmann, J., Kästner, M., 2019. Quantitative assessment of microbial necromass contribution to soil organic matter. Global Change Biology 25, 3578–3590.
Liang, C., Balser, T.C., 2012. Warming and nitrogen deposition lessen microbial residue contribution to soil carbon pool. Nature Communications 3, 1222.
Liang, C., Schimel, J.P., Jastrow, J.D., 2017. The importance of anabolism in microbial control over soil carbon storage. Nature Microbiology 2, 1–6.
Lugato, E., Lavallee, J.M., Haddix, M.L., Panagos, P., Cotrufo, M.F., 2021. Different climate sensitivity of particulate and mineral-associated soil organic matter. Nature Geoscience 14, 295–300.
Luo, Z., Viscarra Rossel, R.A., Shi, Z., 2020. Distinct controls over the temporal dynamics of soil carbon fractions after land use change. Global Change Biology 26, 4614–4625.
Malik, A.A., Puissant, J., Buckeridge, K.M., Goodall, T., Jehmlich, N., Chowdhury, S., Gweon, H.S., Peyton, J.M., Mason, K.E., van Agtmaal, M., Blaud, A., Clark, I.M., Whitaker, J., Pywell, R.F., Ostle, N., Gleixner, G., Griffiths, R.I., 2018. Land use driven change in soil pH affects microbial carbon cycling processes. Nature Communications 9, 3591.
Miltner, A., Bombach, P., Schmidt-Brücken, B., Kästner, M., 2012. SOM genesis: microbial biomass as a significant source. Biogeochemistry 111, 41–55.
Morrissey, E.M., McHugh, T.A., Preteska, L., Hayer, M., Dijkstra, P., Hungate, B.A., Schwartz, E., 2015. Dynamics of extracellular DNA decomposition and bacterial community composition in soil. Soil Biology and Biochemistry 86, 42–49.
Nelson, D.W., Sommers, 1996. Total carbon, organic carbon, and organic matter. In: Sparks, D.L., et al. (Eds.), Methods of Soil Analysis: Part 3. Chemical Methods, Madison, pp. 961–1010.
Rowley, M.C., Grand, S., Verrecchia, É.P., 2018. Calcium-mediated stabilisation of soil organic carbon. Biogeochemistry 137, 27–49.
Six, J., Frey, S.D., Thiet, R.K., Batten, K.M., 2006. Bacterial and fungal contributions to carbon sequestration in agroecosystems. Soil Science Society of America Journal 70, 555–569.
Smith, P., Adams, J., Beerling, D.J., Beringer, T., Calvin, K.V., Fuss, S., Griscom, B., Hagemann, N., Kammann, C., Kraxner, F., Minx, J.C., Popp, A., Renforth, P., Vicente, J.L.V., Keesstra, S., 2019. Land-management options for greenhouse gas removal and their impacts on ecosystem services and the Sustainable Development Goals. Annual Review of Environment and Resources 44, 255–286.
Spawn, S.A., Sullivan, C.C., Lark, T.J., Gibbs, H.K., 2020. Harmonized global maps of above and belowground biomass carbon density in the year 2010. Scientific Data 7, 112.
Spohn, M., Klaus, K., Wanek, W., Richter, A., 2016. Microbial carbon use efficiency and biomass turnover times depending on soil depth – implications for carbon cycling. Soil Biology and Biochemistry 96, 74–81.
Takriti, M., Wild, B., Schnecker, J., Mooshammer, M., Knoltsch, A., Lashchinskiy, N., Eloy Alves, R.J., Gentsch, N., Gittel, A., Mikutta, R., Wanek, W., Richter, A., 2018. Soil organic matter quality exerts a stronger control than stoichiometry on microbial substrate use efficiency along a latitudinal transect. Soil Biology and Biochemistry 121, 212–220.

Tong, X., Brandt, M., Yue, Y., Ciais, P., Rudbeck Jepsen, M., Penuelas, J., Wigneron, J.P., Xiao, X., Song, X., Horion, S., Rasmussen, K., Saatchi, S., Fan, L., Wang, K., Zhang, B., Chen, Z., Wang, Y., Li, X., Fensholt, R., 2020. Forest management in southern China generates short term extensive carbon sequestration. Nature Communications 11, 129.

Wang, C., Qu, L., Yang, L., Liu, D., Morrissey, E., Miao, R., Liu, Z., Wang, Q., Fang, Y., Bai, E., 2021. Large-scale importance of microbial carbon use efficiency and necromass to soil organic carbon. Global Change Biology 27, 2039–2048.

Wang, C., Wang, X., Pei, G.T., Xia, Z.W., Peng, B., Sun, L.F., Wang, J., Gao, D.C., Chen, S. D., Liu, D.W., Dai, W.W., Jiang, P., Fang, Y.T., Liang, C., Wu, N.P., Bai, E., 2020. Stabilization of microbial residues in soil organic matter after two years of decomposition. Soil Biology and Biochemistry 141, 107687.

Wang, K., Zhang, C., Chen, H., Yue, Y., Zhang, W., Zhang, M., Qi, X., Fu, Z., 2019. Karst landscapes of China: patterns, ecosystem processes and services. Landscape Ecology 34, 2743–2763.

Weemstra, M., Peay, K.G., Davies, S.J., Mohamad, M., Itoh, A., Tan, S., Russo, S.E., 2020. Lithological constraints on resource economies shape the mycorrhizal composition of a Bornean rain forest. New Phytologist 228, 253–268.

Wu, J., Joergensen, R.G., Pommerening, B., Chaussod, R., Brookes, P.C., 1990. Measurement of soil microbial biomass C by fumigation-extraction—an automated procedure. Soil Biology and Biochemistry 22, 1167–1169.

Yang, L.M., Lyu, M.K., Li, X.J., Xiong, X.L., Lin, W.S., Yang, Y.S., Xie, J.S., 2020a. Decline in the contribution of microbial residues to soil organic carbon along a subtropical elevation gradient. The Science of the Total Environment 749, 141583.

Yang, S., Jansen, B., Kalbitz, K., Castro, F.O.C., van Hall, R.L., Cammeraat, E.L., 2020b. Lithology controlled soil organic carbon stabilization in an alpine grassland of the Peruvian Andes. Environmental Earth Sciences 79, 66.

Yuan, Y., Li, Y., Mou, Z., Kuang, L., Wu, W., Zhang, J., Wang, F., Hui, D., Peñuelas, J., Sardans, J., Lambers, H., Wang, J., Kuang, Y., Li, Z., Liu, Z., 2020. Phosphorus addition decreases microbial residual contribution to soil organic carbon pool in a tropical coastal forest. Global Change Biology 27, 454–466.

Zhao, Q., Poulson, S.R., Obrist, D., Sumaila, S., Dynes, J.J., McBeth, J.M., Yang, Y., 2016. Iron-bound organic carbon in forest soils: quantification and characterization. Biogeosciences 13, 4777–4788.

Zhu, X., Jackson, R.D., DeLucia, E.H., Tiedje, J.M., Liang, C., 2020. The soil microbial carbon pump: from conceptual insights to empirical assessments. Global Change Biology 26, 6032–6039.